Theses and Dissertations | 1. Thesis and Dissertation Collection, all items

1972

The periodic directional filter.

Tsukada, Kenji.

Monterey, California. Naval Postgraduate School
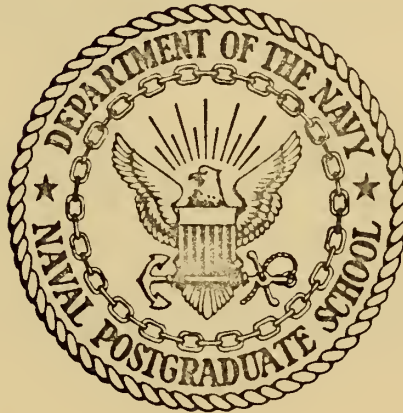
http://hdl.handle.net/10945/16299

THE PERIODIC DIRECTIONAL FILTER

Kenji Tsukada

NAVAL POSTGRADUATE SCHOOL
Monterey, California

THESIS

THE PERIODIC DIRECTIONAL FILTER

by

Kenji Tsukada

Thesis Advisor: J. B. Knorr

September 1972

The Periodic Directional Filter

by

Kenji Tsukada
Lieutenant, Japanese Maritime Self Defense Force
B.S., Chuo University, Japan, 1966

Submitted in partial fulfillment of the
requirements for the degree of

MASTER OF SCIENCE IN ELECTRICAL ENGINEERING

from the
NAVAL POSTGRADUATE SCHOOL
September 1972

ABSTRACT

For the design of the periodic directional filter, some computational aids are required. This thesis describes several useful methods. Various coupling methods are also compared.

In this thesis, only uniform periodic coupling has been examined, but non-uniform periodic coupling may be useful to improve the filter output characteristic. The computer program used in this thesis is available for that purpose.

- 2

TABLE OF CONTENTS

ACKNOWLEDGEMENT

I. INTRODUCTION

Periodically coupled transmission lines have directional characteristics which are useful in applications where filtering and coupling are involved. Figure 1 shows the periodically coupled lines when viewed as a four-port network.
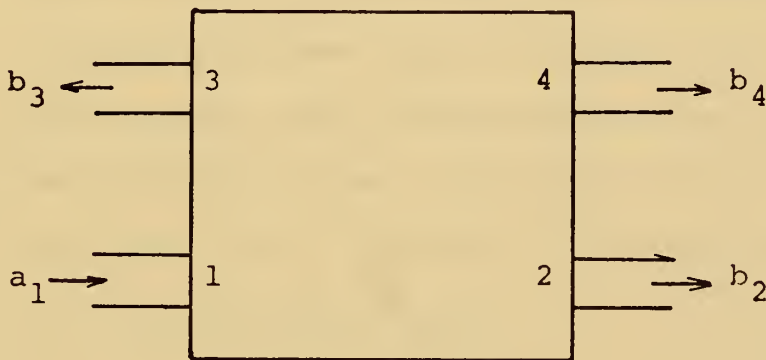
Figure 1

A wave incident upon port 1, the input port, will cause waves to emanate from ports 2, 3 and 4. The energy leaving port 4, however, is only a small percentage of the input energy which is routed mainly to ports 2 and 3. The division of energy between ports 2 and 3 is controlled by the strength of the coupling between the lines and the frequency of interaction depends upon the periodicity. By controlling the coupling between the lines, the network may be made to behave as a bandpass filter (port 1-3), a bandstop filter (port 1-2) or a directional coupler (port 1-3).

5

Several analyses of directional filters have been pub-
lished previously [1], [2]. These authors, however, have
considered resonant rather than traveling wave type struc-
tures. The traveling wave type structure has been analyzed
by J. B. Knorr [3] using the theory of coupled modes. The
purpose of this thesis is to develop an exact method of
analysis for periodically coupled lines.

The equations derived herein are best solved on the
digital computer and a program has been developed for that
purpose. Several different types of filter structures with
uniform coupling have been investigated using this program.
An experimental structure was constructed using microstrip
and the laboratory result obtained with this structure is
compared with the program output.

II.   THE SCATTERING MATRIX OF CASCADED FOUR-PORT NETWORKS

Periodically coupled transmission lines may be considered as cascaded four-port networks. Such networks are most conveniently analyzed using scattering matrices. This section develops two methods for computing the scattering parameters of two cascaded four-port networks. Since a cascade of two four-port is just another four-port, the methods permit the analysis of any arbitrary number of sections.

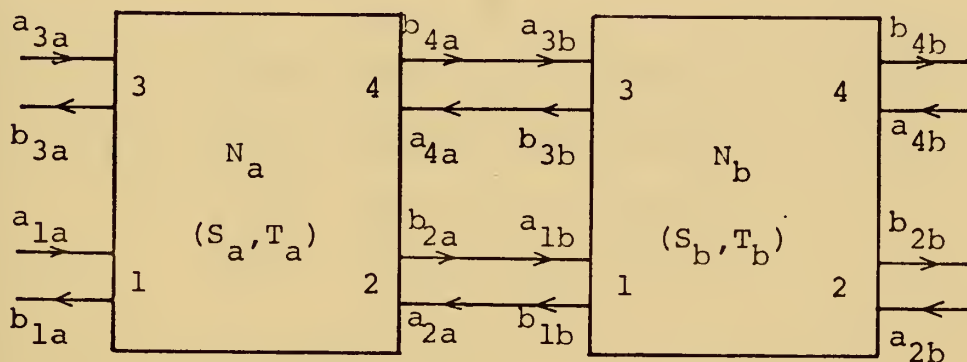The first method of analysis may be developed with reference to Figure 2.

Figure 2

In Figure 2, the scattering matrix S_a for the four-port network, N_a is

$$\begin{pmatrix} b_{1a} \\ b_{2a} \\ b_{3a} \\ b_{4a} \end{pmatrix} = \begin{pmatrix} s_{11a} & s_{12a} & s_{13a} & s_{14a} \\ s_{21a} & s_{22a} & s_{23a} & s_{24a} \\ s_{31a} & s_{32a} & s_{33a} & s_{34a} \\ s_{41a} & s_{42a} & s_{43a} & s_{44a} \end{pmatrix} \begin{pmatrix} a_{1a} \\ a_{2a} \\ a_{3a} \\ a_{4a} \end{pmatrix}$$

Now convert this matrix to the transfer scattering matrix T_a defined by

$$\begin{pmatrix} a_{3a} \\ b_{3a} \\ a_{1a} \\ b_{1a} \end{pmatrix} = T_a \begin{pmatrix} b_{4a} \\ a_{4a} \\ b_{2a} \\ a_{2a} \end{pmatrix}$$

where

$$T_a = \begin{pmatrix} t_{11a} & t_{12a} & t_{13a} & t_{14a} \\ t_{21a} & t_{22a} & t_{23a} & t_{24a} \\ t_{31a} & t_{32a} & t_{33a} & t_{34a} \\ t_{41a} & t_{42a} & t_{43a} & t_{44a} \end{pmatrix} .$$

Then if N_a is cascaded with N_b,

$$\begin{pmatrix} a_{3a} \\ b_{3a} \\ a_{1a} \\ b_{1a} \end{pmatrix} = T_a \begin{pmatrix} b_{4a} \\ a_{4a} \\ b_{2a} \\ a_{2a} \end{pmatrix} = T_a \begin{pmatrix} a_{3b} \\ b_{3b} \\ a_{1b} \\ b_{1b} \end{pmatrix} = T_a T_b \begin{pmatrix} b_{4b} \\ a_{4b} \\ b_{2b} \\ a_{2b} \end{pmatrix} .$$

Likewise, for a cascade of n four-port networks,

$$\begin{pmatrix} a_3 \\ b_3 \\ a_1 \\ b_1 \end{pmatrix} = \prod_{i=1}^{n} T_i \begin{pmatrix} b_4' \\ a_4' \\ b_2' \\ a_2' \end{pmatrix}.$$

Then after cascading n networks, reconvert the T matrix of n cascaded networks to the S matrix. These conversions are tabulated in Table I. This method breaks down when $\Delta = 0$. This happens in case of the short coupled transmission lines as will be described. Also, when Δ becomes small, it is not a practical method for the computer work.

A second method which may be used is described below. This is carried out by calculating the scattering parameters of the two cascaded networks, using the scattering parameters of each section directly. These parameters were derived for the network of Figure 2 and are tabulated in Tables II and III. The derivation is shown in the Appendix. This method can be used when Δ is small or even zero.

TABLE I

S to T		T to S	
t_{11}	$\frac{1}{\Delta}\, s_{21}$	s_{11}	$\frac{1}{\Delta}\,(t_{11}t_{43} - t_{13}t_{41})$
t_{12}	$\frac{1}{\Delta}\,(s_{24}s_{41} - s_{21}s_{44})$	s_{12}	$t_{44} + s_{42}t_{41} + s_{22}t_{43}$
t_{13}	$\frac{1}{\Delta}\,(-s_{41})$	s_{13}	$\frac{1}{\Delta}\,(t_{33}t_{41} - t_{31}t_{43})$
t_{14}	$\frac{1}{\Delta}\,(s_{22}s_{41} - s_{21}s_{42})$	s_{14}	$t_{42} + s_{44}t_{41} + s_{24}t_{23}$
t_{21}	$\frac{1}{\Delta}\,(s_{33}s_{21} - s_{31}s_{23})$	s_{21}	$\frac{1}{\Delta}\, t_{11}$
t_{22}	$s_{34} + s_{31}t_{32} + s_{33}t_{12}$	s_{22}	$\frac{1}{\Delta}\,(t_{14}t_{31} - t_{11}t_{34})$
t_{23}	$\frac{1}{\Delta}\,(s_{31}s_{43} - s_{33}s_{41})$	s_{23}	$\frac{1}{\Delta}\,(-t_{31})$
t_{24}	$s_{32} + s_{31}t_{34} + s_{33}t_{14}$	s_{24}	$\frac{1}{\Delta}\,(t_{12}t_{31} - t_{11}t_{32})$
t_{31}	$\frac{1}{\Delta}\,(-s_{23})$	s_{31}	$\frac{1}{\Delta}\,(t_{11}t_{23} - t_{13}t_{21})$
t_{32}	$\frac{1}{\Delta}\,(s_{23}s_{44} - s_{24}s_{43})$	s_{32}	$t_{24} + s_{42}t_{21} + s_{22}t_{23}$
t_{33}	$\frac{1}{\Delta}\, s_{43}$	s_{33}	$\frac{1}{\Delta}\,(t_{33}t_{21} - t_{31}t_{23})$
t_{34}	$\frac{1}{\Delta}\,(s_{23}s_{42} - s_{22}s_{43})$	s_{34}	$t_{22} + s_{44}t_{21} + s_{24}t_{23}$
t_{41}	$\frac{1}{\Delta}\,(-s_{11}s_{23} + s_{13}s_{21})$	s_{41}	$\frac{1}{\Delta}\,(-t_{13})$
t_{42}	$s_{14} + s_{11}t_{32} + s_{13}t_{12}$	s_{42}	$\frac{1}{\Delta}\,(t_{13}t_{34} - t_{14}t_{33})$
t_{43}	$\frac{1}{\Delta}\,(s_{11}s_{43} - s_{13}s_{41})$	s_{43}	$\frac{1}{\Delta}\, t_{33}$
t_{44}	$s_{12} + s_{11}t_{34} + s_{13}t_{14}$	s_{44}	$\frac{1}{\Delta}\,(t_{13}t_{32} - t_{12}t_{33})$

$$\Delta = s_{21}s_{43} - s_{23}s_{41} \qquad\qquad \Delta = t_{11}t_{33} - t_{13}t_{31}$$

10

TABLE II

s_{11}	$\frac{1}{D}[s_{12a}(c_{31}s_{21a}+c_{32}s_{41a})+s_{14a}(c_{11}s_{21a}+c_{12}s_{41a})] + s_{11a}$
s_{12}	$\frac{1}{D}[s_{12a}(c_{33}s_{12b}+c_{34}s_{32b}) + s_{14a}(c_{13}s_{12b}+c_{14}s_{32b})]$
s_{13}	$\frac{1}{D}[s_{12a}(c_{31}s_{23a}+c_{32}s_{43a})+s_{14a}(c_{11}s_{23a}+c_{12}s_{43a})] + s_{13a}$
s_{14}	$\frac{1}{D}[s_{12a}(c_{33}s_{14b}+c_{34}s_{34b}) + s_{14a}(c_{13}s_{14b}+c_{14}s_{34b})]$
s_{21}	$\frac{1}{D}[s_{21b}(c_{41}s_{21a}+c_{42}s_{41a}) + s_{23b}(c_{21}s_{21a}+c_{22}s_{41a})]$
s_{22}	$\frac{1}{D}[s_{21b}(c_{43}s_{12b}+c_{44}s_{32b})+s_{23b}(c_{23}s_{12b}+c_{24}s_{32b})] + s_{22b}$
s_{23}	$\frac{1}{D}[s_{21b}(c_{41}s_{23a}+c_{42}s_{43a}) + s_{23b}(c_{21}s_{23a}+c_{22}s_{43a})]$
s_{24}	$\frac{1}{D}[s_{21b}(c_{43}s_{14b}+c_{44}s_{34b})+s_{23b}(c_{23}s_{14b}+c_{24}s_{34b})] + s_{24b}$
s_{31}	$\frac{1}{D}[s_{32a}(c_{31}s_{21a}+c_{32}s_{41a})+s_{34a}(c_{11}s_{21a}+c_{12}s_{41a})] + s_{31a}$
s_{32}	$\frac{1}{D}[s_{32a}(c_{33}s_{12b}+c_{34}s_{32b}) + s_{34a}(c_{13}s_{12b}+c_{14}s_{32b})]$
s_{33}	$\frac{1}{D}[s_{32a}(c_{31}s_{23a}+c_{32}s_{43a})+s_{34a}(c_{11}s_{23a}+c_{12}s_{43a})] + s_{33a}$
s_{34}	$\frac{1}{D}[s_{32a}(c_{33}s_{14b}+c_{34}s_{34b}) + s_{34a}(c_{13}s_{14b}+c_{14}s_{34b})]$
s_{41}	$\frac{1}{D}[s_{41b}(c_{41}s_{21a}+c_{42}s_{41a}) + s_{43b}(c_{21}s_{21a}+c_{22}s_{41a})]$
s_{42}	$\frac{1}{D}[s_{41b}(c_{43}s_{12b}+c_{44}s_{32b})+s_{43b}(c_{23}s_{12b}+c_{24}s_{32b})] + s_{42b}$
s_{43}	$\frac{1}{D}[s_{41b}(c_{41}s_{23a}+c_{42}s_{43a}) + s_{43b}(c_{21}s_{23a}+c_{22}s_{43a})]$
s_{44}	$\frac{1}{D}[s_{41b}(c_{43}s_{14b}+c_{44}s_{34b})+s_{43b}(c_{23}s_{14b}+c_{24}s_{34b})] + s_{44b}$

TABLE III

c_{11}	$-s_{31b} - s_{42a}(s_{11b}s_{33b} - s_{13b}s_{31b})$
c_{12}	$-s_{33b} + s_{22a}(s_{11b}s_{33b} - s_{13b}s_{31b})$
c_{13}	$-s_{42a}s_{33b} - s_{22a}s_{31b}$
c_{14}	$-1 + s_{42a}s_{13b} + s_{22a}s_{11b}$
c_{21}	$-s_{44a}s_{31b} - s_{42a}s_{11b}$
c_{22}	$-1 + s_{24a}s_{31b} + s_{22a}s_{11b}$
c_{23}	$-s_{42a} - s_{31b}(s_{22a}s_{44a} - s_{24a}s_{42a})$
c_{24}	$-s_{44a} + s_{11b}(s_{22a}s_{44a} - s_{24a}s_{42a})$
c_{31}	$-s_{11b} + s_{44a}(s_{11b}s_{33b} - s_{13b}s_{31b})$
c_{32}	$-s_{13b} - s_{24a}(s_{11b}s_{33b} - s_{13b}s_{31b})$
c_{33}	$-1 + s_{24a}s_{31b} + s_{44a}s_{33b}$
c_{34}	$-s_{24a}s_{11b} - s_{44a}s_{13b}$
c_{41}	$-1 + s_{42a}s_{13b} + s_{44a}s_{33b}$
c_{42}	$-s_{22a}s_{13b} - s_{24a}s_{33b}$
c_{43}	$-s_{22a} + s_{33b}(s_{22a}s_{44a} - s_{24a}s_{42a})$
c_{44}	$-s_{24a} - s_{13b}(s_{22a}s_{44a} - s_{24a}s_{42a})$

$$D = -1 + s_{24a}s_{31b} + s_{22a}s_{11b} + s_{42a}s_{13b} + s_{44a}s_{33b}$$

$$+ (s_{24a}s_{42a} + s_{22a}s_{44a})(s_{11b}s_{33b} - s_{13b}s_{31b})$$

III. THE SCATTERING MATRIX OF COUPLED LINES AND THE PERIODIC DIRECTIONAL FILTER

In the previous section, two methods were derived to solve cascaded four-port networks. In this section, elements of the scattering matrix of one section of the periodic directional filter are derived. Cascading these networks, the bandpass transfer characteristic, that is $|s_{31}|^2$, is examined for several types of coupling.

First, the coupled transmission lines shown in Figure 3 are examined. These lines are coupled at the center point of each line through a lumped element, Y_c.
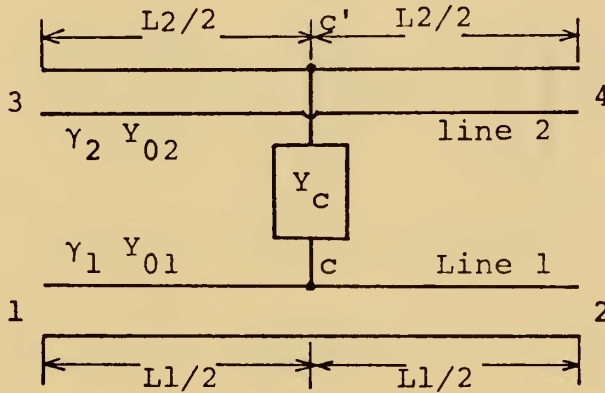

Figure 3

In Figure 3, Y_{01} and Y_{02} are the characteristic admittances of lines 1 and 2 respectively. γ_1 and γ_2 are the propagation constants of each line. Y_c is the coupling admittance between line 1 and line 2. Since this network is reciprocal

13

$$s_{ij} = s_{ji}.$$

Also, the symmetry of the network is such that

$$s_{11} = s_{22},$$
$$s_{33} = s_{44}, \text{ and}$$
$$s_{31} = s_{41} = s_{32} = s_{42}.$$

Thus, s_{11}, s_{21}, s_{31}, s_{33}, s_{43} are the independent matrix elements which must be derived.

To derive these s-parameters, the equivalent circuit for port 1, shown in Figure 4 is used.
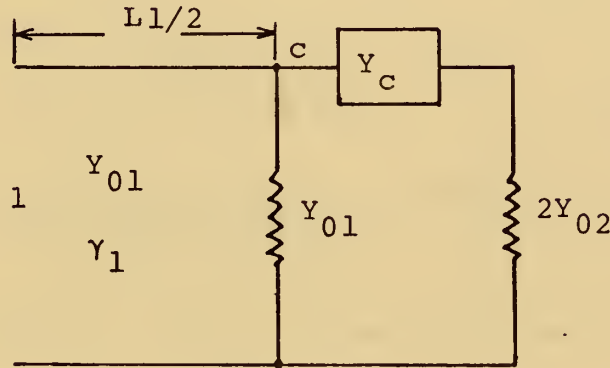

Figure 4

The reflection coefficient at point c is

$$k_{c1} = \frac{Y_{01} - \left(Y_{01} + \dfrac{2Y_{02}Y_c}{2Y_{02}+Y_c} \right)}{Y_{01} + \left(Y_{01} + \dfrac{2Y_{02}Y_c}{2Y_{02}+Y_c} \right)}$$

$$= \frac{-Y_{02}Y_c}{2Y_{01}Y_{02}+Y_c(Y_{01}+Y_{02})}$$

14

so

$$s_{11} = k_{c1} e^{-\gamma_1 L_1} = \frac{-Y_{02} Y_c}{2Y_{01} Y_{02} + Y_c (Y_{01} + Y_{02})} e^{-\gamma_1 L_1}$$

$$s_{21} = (1+k_{c1}) e^{-\gamma_1 L_1} = \frac{(2Y_{02} + Y_c) Y_{01}}{2Y_{01} Y_{02} + Y_c (Y_{01} + Y_{02})} e^{-\gamma_1 L_1}$$

$$s_{31} = (1+k_{c1}) \frac{Y_c}{Y_c + 2Y_{02}} \sqrt{\frac{Y_{02}}{Y_{01}}} e^{-(\gamma_1 L_1 + \gamma_2 L_2)/2}$$

$$= \frac{Y_c \sqrt{Y_{01} Y_{02}}}{2Y_{01} Y_{02} + Y_c (Y_{01} + Y_{02})} e^{-(\gamma_1 L_1 + \gamma_2 L_2)/2}$$

Similarly s_{33} and s_{43} are

$$s_{33} = \frac{-Y_{01} Y_c}{2Y_{01} Y_{02} + Y_c (Y_{01} + Y_{02})} e^{-\gamma_2 L_2}$$

$$s_{43} = \frac{(2Y_{01} + Y_c) Y_{02}}{2Y_{01} Y_{02} + Y_c (Y_{01} + Y_{02})} e^{-\gamma_2 L_2}$$

Some interesting relations are found using these scattering parameters. For example,

$$s_{11} s_{33} - s_{13} s_{31} = 0$$

and

$$s_{22} s_{44} - s_{24} s_{42} = 0 .$$

Also, when $Y_c = \infty$

$$\Delta = s_{21} s_{43} - s_{23} s_{41} = 0 .$$

Thus the T matrix method can not be used. However, short coupling is not practical as will be described later.

Now, consider the scattering parameters for periodically coupled lines composed of sections as illustrated in Figure 3.

First, consider the case where the lines are capacitively coupled with $Y_C = j\omega C$. Y_{01} and Y_{02} are assumed to be G_{01}, G_{02}, that is, pure conductive. This case seems to be very simple, but in some actual cases, it is an appropriate model.

In this case, the scattering parameters are as follows:

$$S_{11} = \frac{-j\omega C \; G_{02}}{2G_{01}G_{02}+j\omega C(G_{01}+G_{02})} \; e^{-(\alpha_1+j\beta_1)L_1}$$

$$S_{21} = \frac{(2G_{02}+j\omega C)G_{01}}{2G_{01}G_{02}+j\omega C(G_{01}+G_{02})} \; e^{-(\alpha_1+j\beta_1)L_1}$$

$$S_{33} = \frac{-j\omega C \; G_{01}}{2G_{01}G_{02}+j\omega C(G_{01}+G_{02})} \; e^{-(\alpha_2+j\beta_2)L_2}$$

$$S_{43} = \frac{(2G_{01}+j\omega C)G_{02}}{2G_{01}G_{02}+j\omega C(G_{01}+G_{02})} \; e^{-(\alpha_2+j\beta_2)L_2}$$

where

α_1 = attenuation coefficient of line 1

α_2 = attenuation coefficient of line 2

β_1 = phase constant of line 1

β_2 = phase constant of line 2

Let $\qquad G_{01} = G_{02}$

$\qquad \omega_0 C = \frac{1}{n} G_{01} \qquad (n = 5,10)$

when

$\qquad \beta_1 L_1 + \beta_2 L_2 = 2\pi$

16

also

$$\alpha_1 = \alpha_2 = 0$$

$$\beta_2 L_2 = 2\beta_1 L_1$$

$$NS = 10, 20, 30$$

where NS is the number of coupled sections. Given these values, the output characteristic of the bandpass directional filter in which the two lines are coupled periodically and uniformly is shown on graphs 1 and 2 which were generated using the computer program. The assumption that $\alpha = 0$ is not practical, but these graphs give some characteristics: (1) The center frequency of this filter deviates from that predicted, if phase shift due to coupling is ignored, in this case, $\beta_1 L_1 = 120°$. (2) When the coupling increases, the bandwidth increases and insertion loss decreases. (3) Insertion loss decreases as the number of sections is increased. In the practical case, the decrease in insertion loss will ultimately be limited by line losses. If a narrow bandpass filter is desired, the coupling should be small and many sections are needed. Then the insertion loss at the center frequency of the filter increases because of line losses.

As a second example, consider the case that $Y_c = \infty$, that is short coupling. The scattering parameters for this condition are

$$S_{11} = \frac{-G_{02}}{G_{01} + G_{02}} e^{-(\alpha_1 + j\beta_1)L_1}$$

17

$$s_{21} = \frac{G_{01}}{G_{01} + G_{02}} \, e^{-(\alpha_1 + j\beta_1)L_1}$$

$$s_{33} = \frac{-G_{01}}{G_{01} + G_{02}} \, e^{-(\alpha_2 + j\beta_2)L_2}$$

$$s_{43} = \frac{G_{02}}{G_{01} + G_{02}} \, e^{-(\alpha_2 + j\beta_2)L_2}$$

$$s_{31} = \frac{\sqrt{G_{01}G_{02}}}{G_{01} + G_{02}} \, e^{-(\alpha_1 + j\beta_1)L_1/2 \, - \, (\alpha_2 + j\beta_2)L_2/2}$$

Graph 3 shows the computer program output for the fol-
lowing values:

$$G_{01} = G_{02} = 0.02 \; [\mho]$$
$$v_1 = v_2 = 2.08 \times 10^8 \; [m/sec]$$
$$\alpha_1 = \alpha_2 = 0.3 \; [1/m]$$
$$L_1 = 0.018 \; [m]$$
$$L_2 = 0.034 \; [m]$$
$$NS = 10$$

where v_1 and v_2 are the wave propagation velocities on the
line 1 and the line 2 respectively. Another filter is
shown in graph 4. Here,

$$G_{01} = 0.02 \; [\mho]$$
$$G_{02} = 0.01 \; [\mho]$$
$$v_1 = v_2 = 2.08 \times 10^8 \; [m/sec]$$
$$L_1 = 0.018 \; [m]$$
$$L_2 = 0.018 \; [m]$$
$$\alpha_1 = \alpha_2 = 0.03 \; [1/m]$$
$$NS = 10$$

In graph 3, the output characteristic is smooth, but the band width is very wide. This is caused by the large coupling. To reduce the coupling, G_{02} is reduced by one half for the filter shown in graph 4. However in this example, the output is distorted as observed on graph 4. This may happen because the reflection coefficient on line 2 increases and is unbalanced with that on line 1. This characteristic appears whenever $G_{01} \neq G_{02}$. Thus the short-coupled periodic filter does not appear to have desirable characteristics.

So far, two coupling methods have been examined, one by the capacitance, another by short. Only the former appears practical.

The next method to be considered is a little different from the previous methods and is shown in Figure 5. The lines are coupled here by means of intermediate transmission line. The practical merit of this method is that direct coupling can be used. This type of filter is easier to construct for this reason.
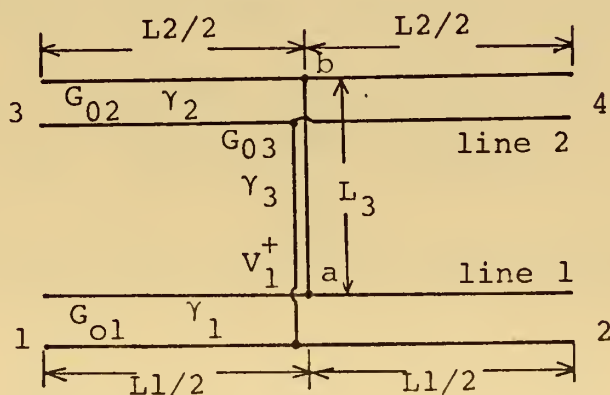

Figure 5

This configuration is the same as Figure 3 except a transmission line is used for coupling. To derive the scattering parameters of this network, it is convenient to redraw it as follows:
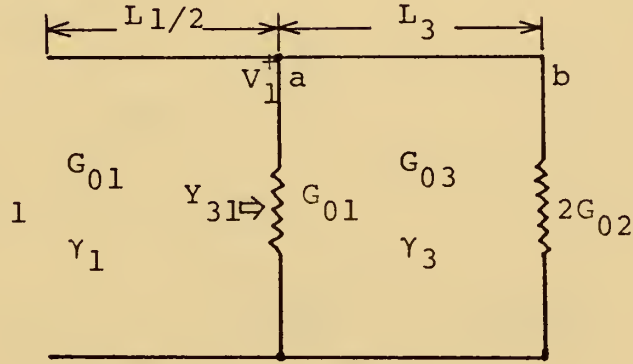

Figure 6

where G_{03} is the characteristic admittance of the coupling line

γ_3 is the propagation constant of the coupling line

V_1^+ is the incident voltage wave at point a

V_b is the voltage at point b.

In this network, the input admittance Y_{31} at point a is

$$Y_{31} = G_{01} + \frac{e^{\gamma_3 L_3} - k_{rb1}\, e^{-\gamma_3 L_3}}{e^{\gamma_3 L_3} + k_{rb1}\, e^{-\gamma_3 L_3}}\, G_{03}$$

where k_{rb1} is the reflection coefficient at point b and is given as

$$k_{rb1} = \frac{G_{03} - 2G_{02}}{G_{03} + 2G_{02}}$$

Also, the reflection coefficient at point a is

$$k_{ra1} = \frac{G_{01} - Y_{31}}{G_{01} + Y_{31}}$$

Thus

$$s_{11} = k_{ra1}\, e^{-\gamma_1 L_1}$$

$$s_{21} = (1 + k_{ra1})\, e^{-\gamma_1 L_1}$$

The voltage at b is given by

$$V_b = \frac{2(1+k_{ra1})V_1^+}{(1+2G_{02}/G_{03})(e^{\gamma_3 L_3} + k_{rb1}\, e^{-\gamma_3 L_3})}$$

hence,

$$s_{31} = \frac{V_b}{V_{+1}}\sqrt{\frac{G_{02}}{G_{01}}}\; e^{-(\gamma_1 L_1 + \gamma_2 L_2)/2}$$

$$= \frac{2(1+k_{ra1})}{(1+2G_{02}/G_{03})(e^{\gamma_3 L_3} + k_{rb1}\, e^{-\gamma_3 L_3})}\sqrt{\frac{G_{02}}{G_{01}}}\; e^{-(\gamma_1 L_1 + \gamma_2 L_2)/2}$$
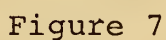
Similarly, in Figure 7,

$$k_{ra2} = \frac{G_{03} - 2G_{01}}{G_{03} + 2G_{01}}\;,$$

$$Y_{32} = G_{02} + \frac{e^{\gamma_3 L_3} - k_{ra2}\, e^{-\gamma_3 L_3}}{e^{\gamma_3 L_3} + k_{ra2}\, e^{-\gamma_3 L_3}}\; G_3\;,$$

$$k_{rb2} = \frac{G_{02} - Y_{32}}{G_{02} + Y_{32}}\;,$$

$$s_{33} = k_{rb2}\, e^{-\gamma_2 L_2}$$

21

Figure 7

and

$$s_{43} = (1 + k_{rb2})\ e^{-\gamma_2 L_2}$$

In these circuits, Y_{31} and Y_{32} can be capacitive, inductive or conductive depending on the length of L_3

$L_3 < \lambda/4$; inductive

$L_3 = \lambda/4$; conductive

$L_3 > \lambda/4$; capacitive

Let $L_3 = \lambda/4$ at the desired center frequency. For computational purposes, the following values were used in the computer program:

$L_1 = 0.018$ [m]

$L_2 = 0.034$ [m]

$\lambda = L_1 + L_2$ at the center frequency

then

$L_3 = \lambda/4 = 0.013$ [m] .

22

Also, let

$$G_{02} = G_{01} = 0.02 \ [\mho]$$

$$G_{03} = 0.007 \ [\mho]$$

$$v_1 = v_2 = 2.08 \times 10^8 \ [m]$$

$$\alpha_1 = \alpha_2 = 0.3 \ [1/m]$$

$$\alpha_3 = 0.5 \ [1/m]$$

$$NS = 10$$

For these values, the computer output is shown on graph 5. The bandwidth is decreased, but more sections are necessary to minimize insertion loss. The other merits of this method are as follows: (1) The value of each parameter can be obtained easily for the desired filter. (2) When $L_3 = \lambda/4$, the center frequency does not deviate from the expected value since the coupling introduces no phase shift. (3) The characteristics of the directional filter can be changed by changing only L_3 and G_{03}. So, any kind of band pass characteristic should be possible by merely changing the length and width of line 3 from section to section. (4) There is no matching problem because G_{01} and G_{02} can be adjusted to the characteristic admittances of the outer circuit. A practical defect of this type coupling is that the insertion of line 3 makes losses larger. When narrow bandwidth is desired, the width of line 3 becomes narrow and this causes more loss also. However, this seems to be a very practical geometry for constructing directional filters using microstrips.

IV. EXPERIMENT

Two practical methods of coupling have been described, capacitive and quarter wave. Although it would have been desirable to examine both methods, time limitations allowed investigation of only the capacitive coupling method. The structure of the filter is shown in Figure 8. The characteristic impedances of line 1 and line 2 are Z_{01} = 50Ω and Z_{02} = 150Ω respectively. The capacitance between the lines was calculated as

$$C = \frac{1}{Z_{02c} \, v_c} = 0.1 \text{ [PF]}$$

where

Z_{02c} = the impedance of line 2 in the coupling region

v_c = the wave velocity of line 2 in the coupling region

The propagation velocities on the lines 1 and 2 are
v_1 = 2.08 x 10^8 [m/sec], v_2 = 2.23 x 10^8 [m/sec]
α_1 = 0.3 [1/m], α_2 = 0.7 [1/m] were found by measurement and
NS = 20.

The computational result using these values is compared with the experimental output in graph 6. There were some practical difficulties encountered in the construction of this filter; (1) the etching of the narrow line, here line 2. (2) the placement of line 2 on the center line of the filter so as to create a glide symmetric structure. (3) the
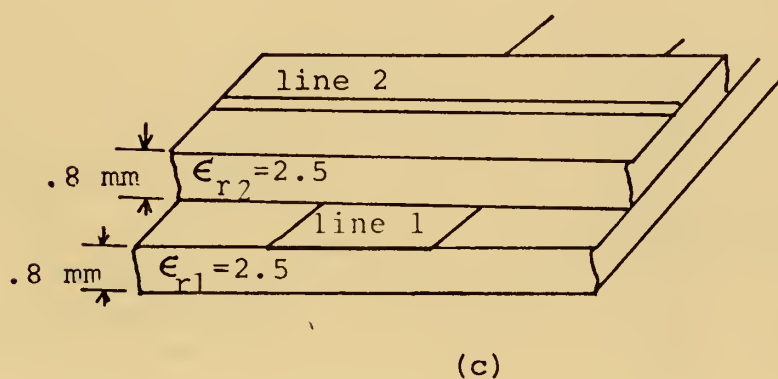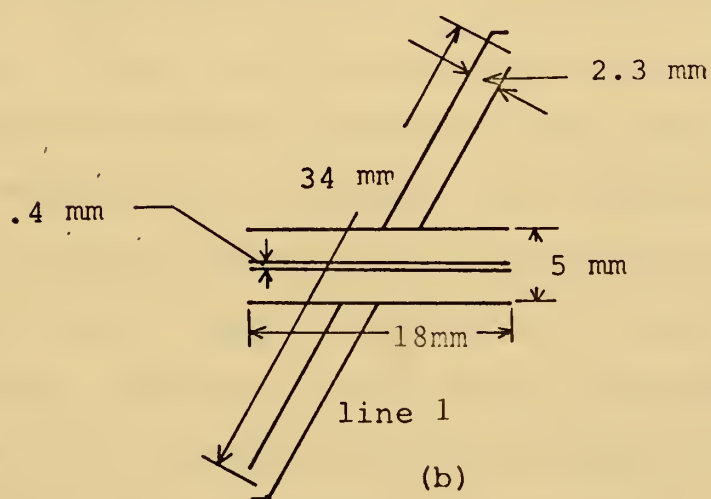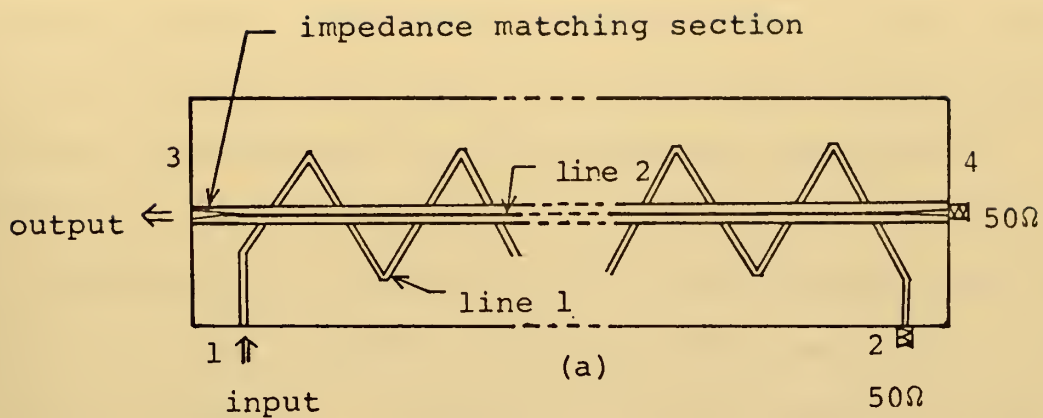
24

impedance matching section

3

output ⇐

line 2

line 1

1 ⇑

input

4

50Ω

2

50Ω

(a)

2.3 mm

34 mm

.4 mm

5 mm

18mm

line 1

(b)

line 2

.8 mm ϵ_{r2}=2.5

line 1

.8 mm ϵ_{r1}=2.5

(c)

Figure 8

25

matching between line 2 and the output line. Also, some
uncertain factors existed; for example, the value of the
coupling capacitance and the propagation velocity of
line 2.

Considering the uncertainty of these factors, the theo-
retical and experimental results probably agree as well as
could be expected. In general, the experimental results
show a wide bandwidth because of the width of the micro
strip line. Better construction techniques would probably
have resulted in better agreement between experiment and
theory. Characteristic impedance and coupling capacitance
cannot be changed independently in this filter as the two
are interrelated. Several possibilities exist for solving
this problem. One method uses the gap capacitance as shown
in Figure 9(a). The same plane can be used in this method.
Another method is illustrated in Figure 9(b).
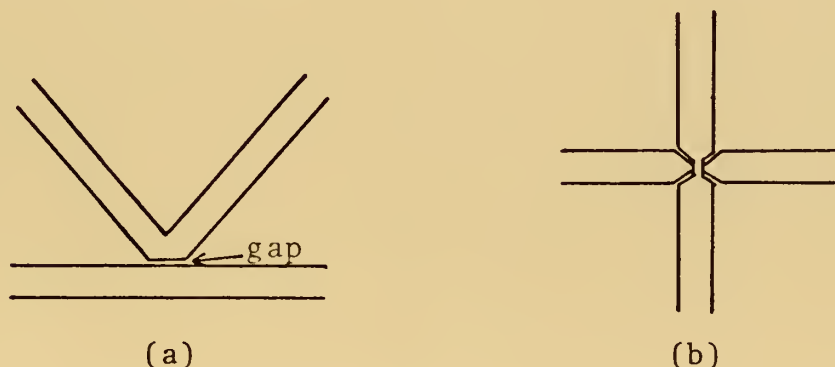

(a)   (b)

Figure 9

In any event, there are some difficulties in coupling lines
with capacitance. However, this method has less loss than
the method in which the transmission line is used to couple.
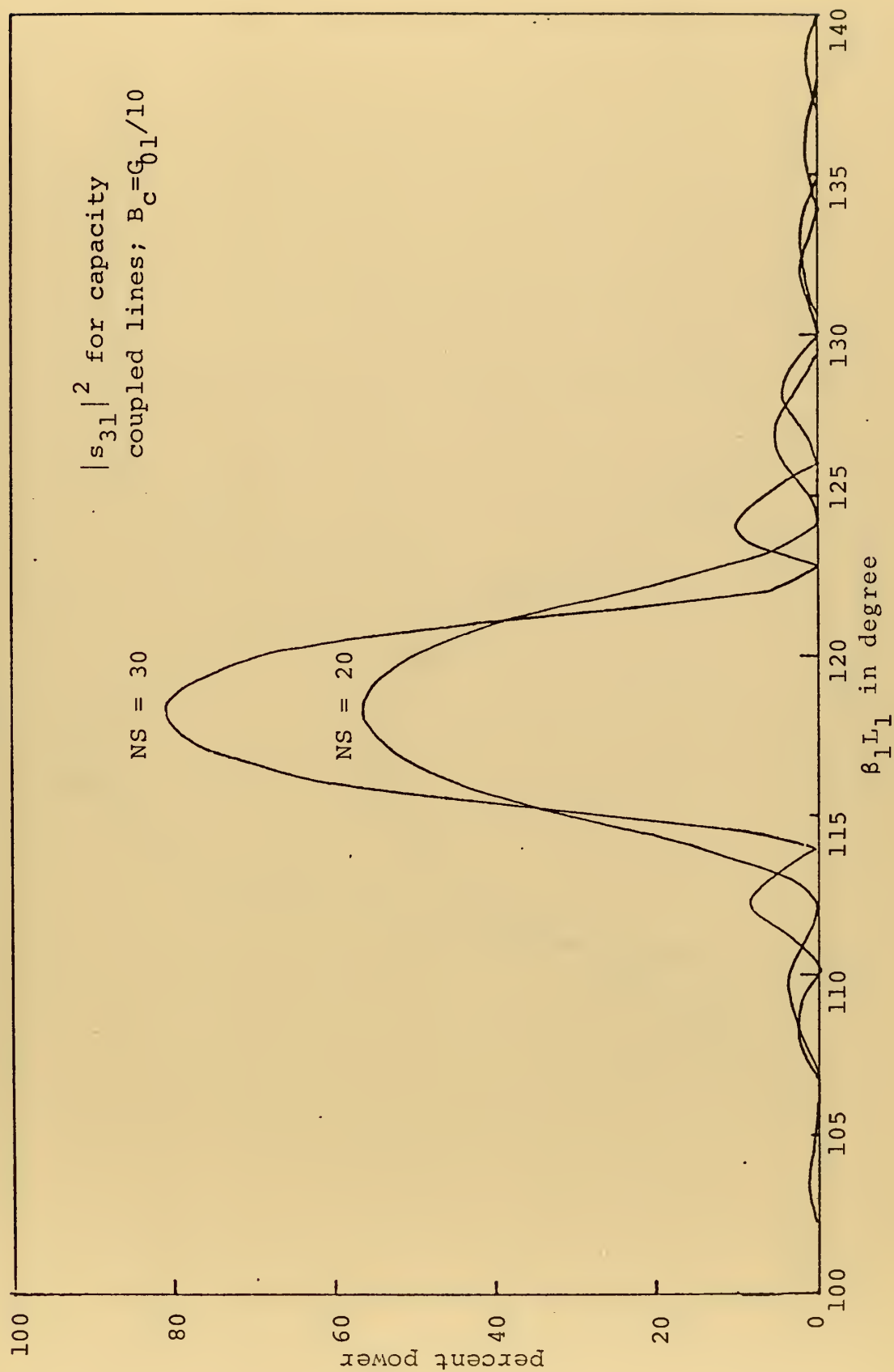Both methods are useful practically.

V. SUMMARY

This thesis has presented computational methods for the analysis of periodically coupled transmission lines. Two methods have been described for obtaining the scattering matrix of two cascaded four-port networks where the S-matrix of the individual networks are known. One method utilizes the scattering transfer matrix and the other method gives the elements of the scattering matrix directly in terms of the elements of the matrices of the individual networks.

The computer program which was developed in the course of this investigation has been used to examine the response characteristics of lines coupled by various means. .Coupling by capacitance or by quarter wavelength sections appears most practical. Each method, however, has advantages and disadvantages. The merit of the former is its lower loss, but its realization is more difficult. The later method appears promising because of the ease of construction.
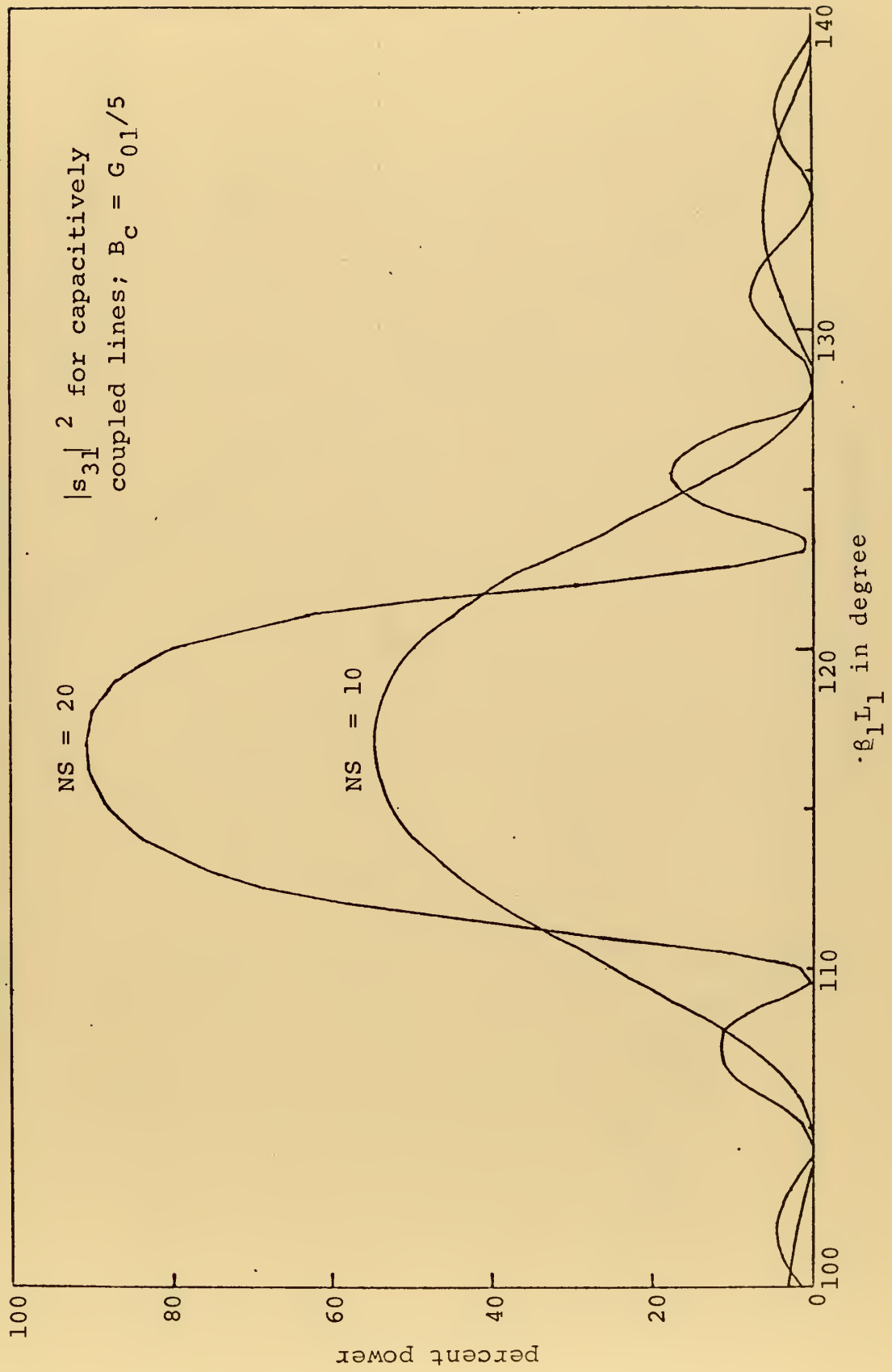
In this thesis, only uniformly coupled lines were investigated. The strength of the coupling was such that considerable transfer of energy occurred, giving the net-work a filter type response rather than a directional coupler type response. Periodically coupled lines should also be useful as directional couplers, however. It is expected that techniques involving non-uniform coupling

and log periodic coupling will be useful for controlling
the response of periodic directional couplers. The computer
program developed in this investigation may be used for
further studies in these areas.

GRAPH 1

$|s_{31}|^2$ for capacity coupled lines; $B_c = G_{01}/10$

NS = 30

NS = 20

percent power

$\beta_1 L_1$ in degree

30

GRAPH 2

$|s_{31}|^2$ for capacitively
coupled lines; $B_c = G_{01}/5$

NS = 20

NS = 10

$\cdot \beta_1 L_1$ in degree

percent power

100
80
60
40
20

100   110   120   130   140

31

GRAPH 3

$|s_{31}|^2$ for short coupled lines: $G_{01}=G_{02}$

percent power

frequency in gigahertz

GRAPH 4

$|s_{31}|^2$ for short
coupled lines: $G_{01} \neq G_{02}$

frequency in gigahertz

percent power

33

GRAPH 5

$|s_{31}|^2$ for directly coupled lines

frequency in gigahertz

percent power

34

GRAPH 6

comparison of $|s_{31}|^2$ between experimental and theoretical results

EXPERIMENTAL

THEORETICAL

frequency in gigahertz

percent power

100

80

60

40

20

0

3.0

3.5

4.0

4.5

5.0
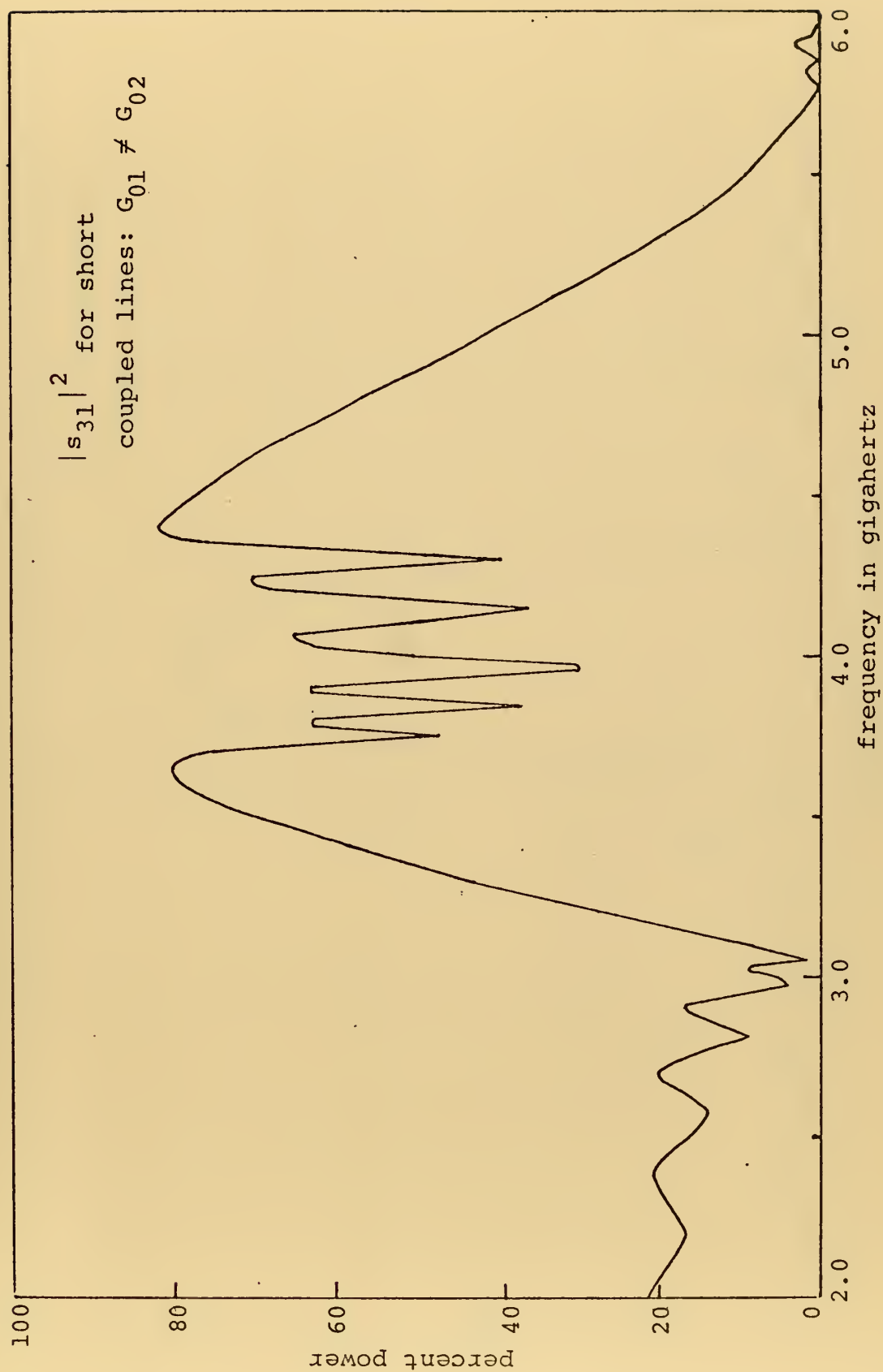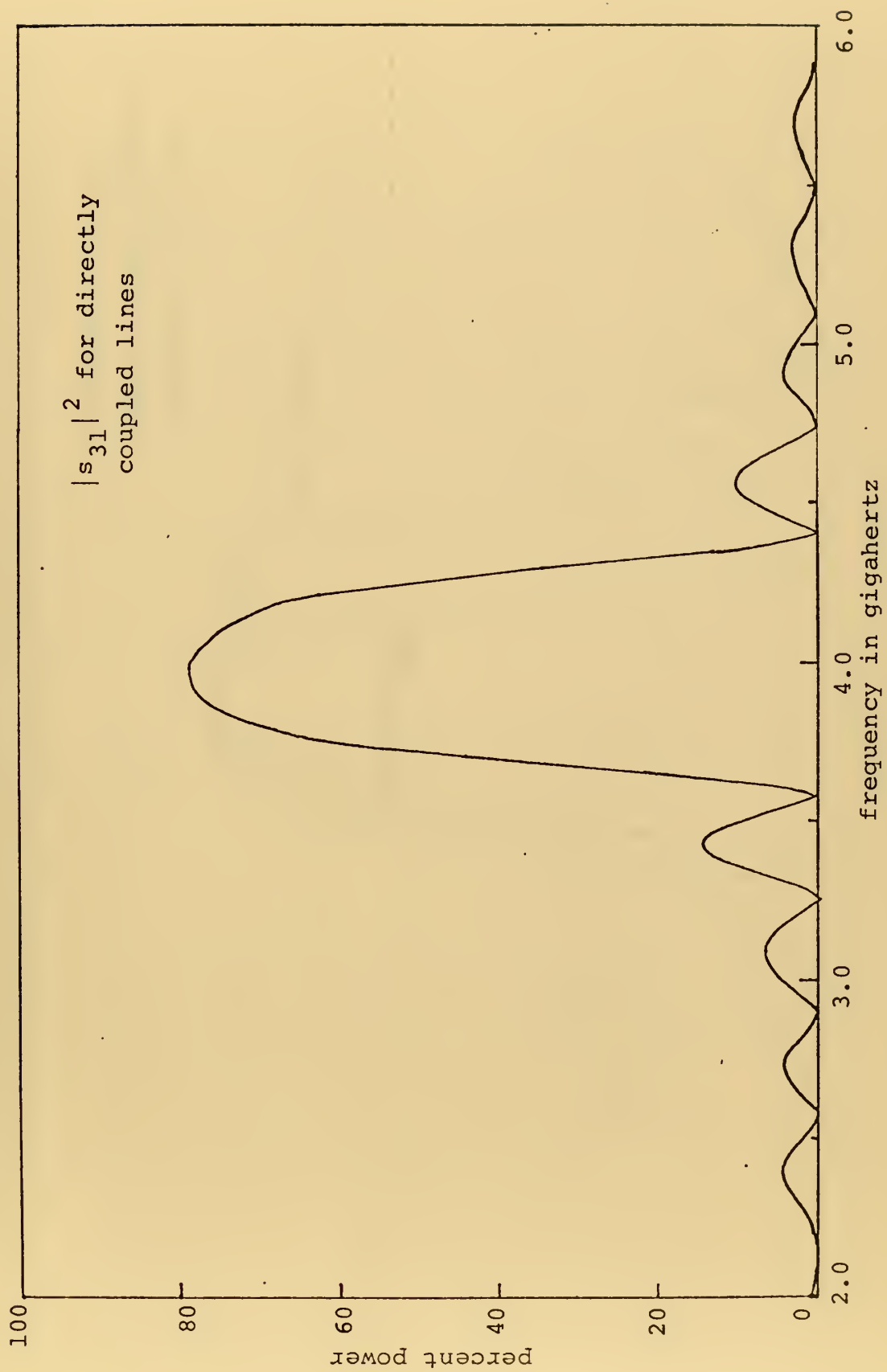
35
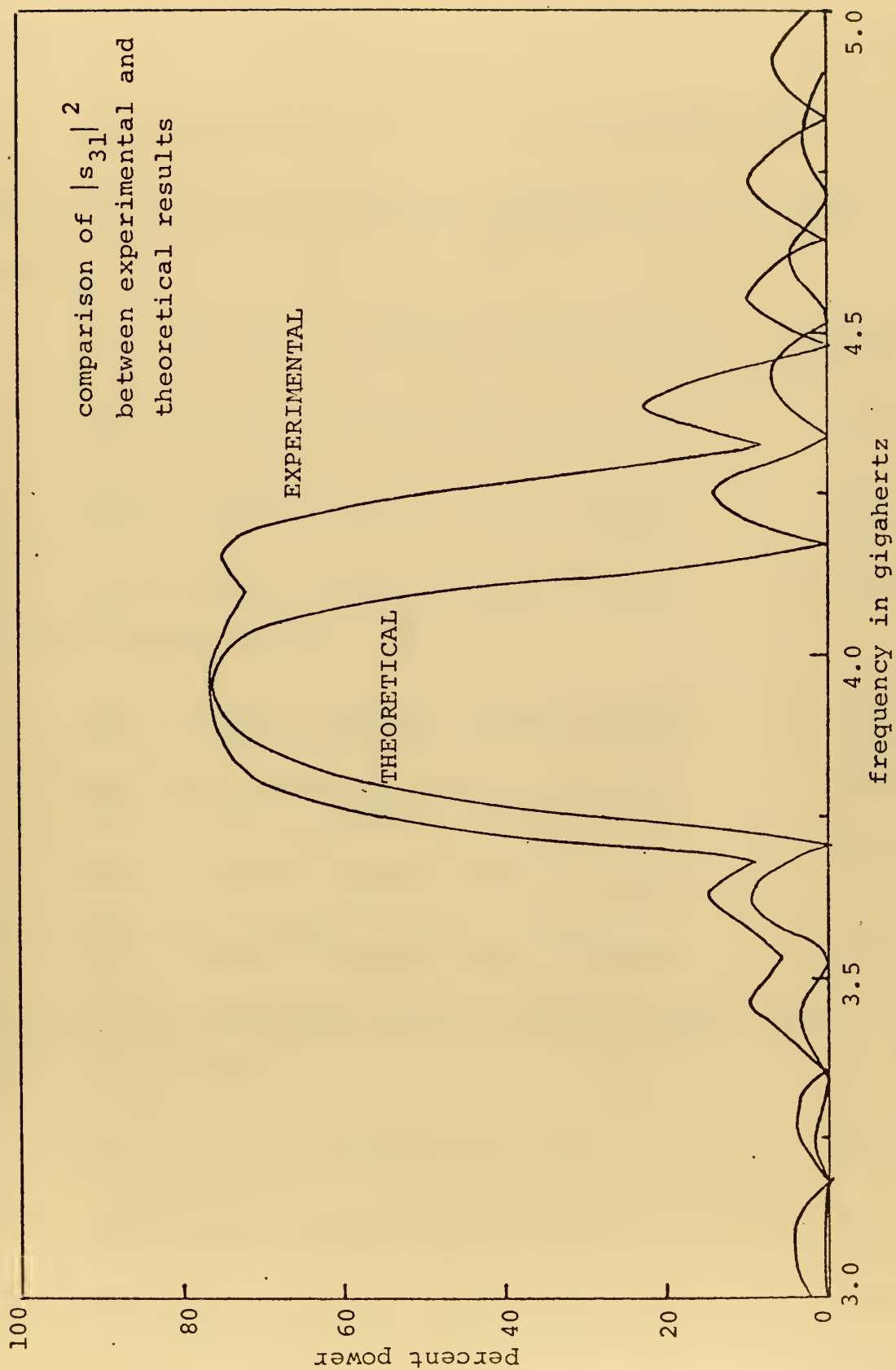
APPENDIX

THE SCATTERING MATRIX OF THE CASCADED NETWORK

On the Figure 2, the scattering parameters of the network Na are

$$b_{1a} = s_{11a}a_{1a} + s_{12a}a_{2a} + s_{13a}a_{3a} + s_{14a}a_{4a} \qquad (A.1)$$

$$b_{2a} = s_{21a}a_{1a} + s_{22a}a_{2a} + s_{23a}a_{3a} + s_{24a}a_{4a} \qquad (A.2)$$

$$b_{3a} = s_{31a}a_{1a} + s_{32a}a_{2a} + s_{33a}a_{3a} + s_{34a}a_{4a} \qquad (A.3)$$

$$b_{4a} = s_{41a}a_{1a} + s_{42a}a_{2a} + s_{43a}a_{3a} + s_{44a}a_{4a} \qquad (A.4)$$

also for the network Nb.

$$b_{1b} = s_{11b}a_{1b} + s_{12b}a_{2b} + s_{13b}a_{3b} + s_{14b}a_{4b} \qquad (A.5)$$

$$b_{2b} = s_{21b}a_{1b} + s_{22b}a_{2b} + s_{23b}a_{3b} + s_{24b}a_{4b} \qquad (A.6)$$

$$b_{3b} = s_{31b}a_{1b} + s_{32b}a_{2b} + s_{33b}a_{3b} + s_{34b}a_{4b} \qquad (A.7)$$

$$b_{4b} = s_{41b}a_{1b} + s_{42b}a_{2b} + s_{43b}a_{3b} + s_{44b}a_{4b} \qquad (A.8)$$

The scattering parameters of the cascaded network can be expressed as follows:

$$b_{1a} = s_{11}a_{1a} + s_{12}a_{2b} + s_{13}a_{3a} + s_{14}a_{4b} \qquad (A.9)$$

$$b_{2b} = s_{21}a_{1a} + s_{22}a_{2b} + s_{23}a_{3a} + s_{24}a_{4b} \qquad (A.10)$$

$$b_{3a} = s_{31}a_{1a} + s_{32}a_{2b} + s_{33}a_{3a} + s_{34}a_{4b} \qquad (A.11)$$

$$b_{4b} = s_{41}a_{1a} + s_{42}a_{2b} + s_{43}a_{3a} + s_{44}a_{4b} \qquad (A.12)$$

Now let $b_{1b} = a_{2a}$, $b_{3b} = a_{4a}$, $a_{1b} = b_{2a}$, $a_{3b} = b_{4a}$, in (A.5), (A.6), (A.7), (A.8)

$$a_{2a} = s_{11b}b_{2a} + s_{12b}a_{2b} + s_{13b}b_{4a} + s_{14b}a_{4b} \tag{A.13}$$

$$b_{2b} = s_{21b}b_{2a} + s_{22b}a_{2b} + s_{23b}b_{4a} + s_{24b}a_{4b} \tag{A.14}$$

$$a_{4a} = s_{31b}b_{2a} + s_{32b}a_{2b} + s_{33b}b_{4a} + s_{34b}a_{4b} \tag{A.15}$$

$$b_{4b} = s_{41b}b_{2a} + s_{42b}a_{2b} + s_{43b}b_{4a} + s_{44b}a_{4b} \tag{A.16}$$

In these equations and (A.1), (A.2), (A.3), (A.4), to eliminate a_{2a}, b_{2a}, a_{4a}, b_{4a}, first derive these values from (A.2), (A.4), (A.13), (A.15)

$$b_{2a} = s_{21a}a_{1a} + s_{22a}a_{2a} + s_{23a}a_{3a} + s_{24a}a_{4a} \tag{A.2}$$

$$b_{4a} = s_{41a}a_{1a} + s_{42a}a_{2a} + s_{43a}a_{3a} + s_{44a}a_{4a} \tag{A.4}$$

$$a_{2a} = s_{11b}b_{2a} + s_{12b}a_{2b} + s_{13b}b_{4a} + s_{14b}a_{4b} \tag{A.13}$$

$$a_{4a} = s_{31b}b_{2a} + s_{32b}a_{2b} + s_{33b}b_{4a} + s_{34b}a_{4b} \tag{A.15}$$

Now set these equations in the form as follows

$$A \begin{pmatrix} a_{4a} \\ b_{4a} \\ a_{2a} \\ b_{2a} \end{pmatrix} = B \begin{pmatrix} a_{1a} \\ a_{2b} \\ a_{3a} \\ a_{4b} \end{pmatrix} \tag{A.16}$$

where

$$A = \begin{pmatrix} -s_{24a} & 0 & -s_{22a} & 1 \\ -s_{44a} & 1 & -s_{42a} & 0 \\ 0 & -s_{13b} & 1 & -s_{11b} \\ 1 & -s_{33b} & 0 & -s_{31b} \end{pmatrix} \tag{A.17}$$

$$B = \begin{pmatrix} s_{21a} & 0 & s_{23a} & 0 \\ s_{41a} & 0 & s_{43a} & 0 \\ 0 & s_{12b} & 0 & s_{14b} \\ 0 & s_{32b} & 0 & s_{34b} \end{pmatrix} \qquad (A.18)$$

To solve this equation, derive the inverse of the matrix A

$$C = A^{-1} = \frac{1}{D}\begin{pmatrix} c_{11} & c_{12} & c_{13} & c_{14} \\ c_{21} & c_{22} & c_{23} & c_{24} \\ c_{31} & c_{32} & c_{33} & c_{34} \\ c_{41} & c_{42} & c_{43} & c_{44} \end{pmatrix} \qquad (A.19)$$

where $D = |A|$

These values are tabulated in Table II. Then

$$\begin{pmatrix} a_{4a} \\ b_{4a} \\ a_{2a} \\ b_{2a} \end{pmatrix} = CB \begin{pmatrix} a_{1a} \\ a_{2b} \\ a_{3a} \\ a_{4b} \end{pmatrix} \qquad (A.20)$$

After getting a_{4a}, b_{4a}, a_{2a}, b_{2a}, substitute these values into (A.1), (A.3), (A.6), (A.8). Then rearrange those equations as (A.9), (A.10), (A.11), (A.12).

BIBLIOGRAPHY

1. Cohn, S. B. and Coale, F. S., Directional Channel-
    Separation Fileers, Proceeding of the IRE,
    p. 1018-1024, August 1956.

2. Wanselow, R. D. and Tuttle, L. P., Jr., Practical
    Design of Strip-Transmission-Line Half-Wavelength
    Resonator Directional Filters, IRE Transaction on
    Microwave Theory and Techniques, p. 168-173,
    January 1959.

3. Knorr, J. B., Periodic Coupling of Modes of Propega-
    tion, Naval Postgraduate School-52K 071081A,
    August 1971.

INITIAL DISTRIBUTION LIST

No. Copies

1. Defense Documentation Center   2
    Cameron Station
    Alexandria, Virginia   22314

2. Library, Code 0212   2
    Naval Postgraduate School
    Monterey, California   93940

3.. Asst. Professor J. B. Knorr   1
    Department of Electrical Engineering
    Naval Postgraduate School
    Monterey, California   93940

4. LT Kenji Tsukada, JMSDF   1
    4-11-24 Minamiazabu, Minato-Ku
    Tokyo, Japan

DOCUMENT CONTROL DATA - R & D

(Security classification of title, body of abstract and indexing annotation must be entered when the overall report is classified)

1. ORIGINATING ACTIVITY *(Corporate author)*	2a. REPORT SECURITY CLASSIFICATION
Naval Postgraduate School Monterey, California 93940	Unclassified
	2b. GROUP

3. REPORT TITLE

THE PERIODIC DIRECTIONAL FILTER

4. DESCRIPTIVE NOTES *(Type of report and inclusive dates)*

Master's Thesis; September 1972

5. AUTHOR(S) *(First name, middle initial, last name)*

Kenji Tsukada; Lieutenant, Japanese Maritime Self Defense Force

6. REPORT DATE	7a. TOTAL NO. OF PAGES	7b. NO. OF REFS
September 1972	42	3

8a. CONTRACT OR GRANT NO.	9a. ORIGINATOR'S REPORT NUMBER(S)
b. PROJECT NO.	
c.	9b. OTHER REPORT NO(S) *(Any other numbers that may be assigned this report)*
d.	

10. DISTRIBUTION STATEMENT

Approved for public release; distribution unlimited

11. SUPPLEMENTARY NOTES	12. SPONSORING MILITARY ACTIVITY
	Naval Postgraduate School Monterey, California 93940

13. ABSTRACT

For the design of the periodic directional filter, some computational aids are required. This thesis describes several useful methods. Various coupling methods are also compared.

In this thesis, only uniform periodic coupling has been examined, but non-uniform periodic coupling may be useful to improve the filter output characteristic. The computer program used in this thesis is available for that purpose.

DD FORM 1473 (PAGE 1)
1 NOV 65

S/N 0101-807-6811

41

A-31408

14. KEY WORDS	LINK A		LINK B		LINK C	
	ROLE	WT	ROLE	WT	ROLE	WT

.